JEE Journal of Ecological Engineering

Journal of Ecological Engineering, 2025, 26(9), 281–296
https://doi.org/10.12911/22998993/205185
ISSN 2299–8993, License CC-BY 4.0

Received: 2025.05.06
Accepted: 2025.06.13
Published: 2025.06.23

Thermal environmental characteristics and their regulation mechanisms of three typical urban land-use types in Guangzhou, South China

Gang Wang[1,2*], Ling Xiao[3], Zifeng Liang[1], Ziyin Huang[2], Dongsheng Guan[2]

[1] School of Management, Guangdong University of Technology, Guangzhou 510520, China
[2] School of Environmental Science and Engineering, Sun Yat-sen University, Guangzhou 510275, China
[3] Department of Materials and Environmental Engineering, Shantou University, Shantou 515063, China
* Corresponding author's e-mail: gdut_tony@163.com

ABSTRACT

Recent studies highlight accelerated urbanization and industrialization significantly influence urban heat islands (UHIs). In Guangzhou, South China, three typical land-use types (e.g. urban village, residential district, and urban park) were selected to study their thermal characteristics and regulation mechanisms. Land surface temperature (LST) retrieved from Landsat 8 image was used to quantify UHI effects. The result showed that the minimum, maximum and average values of LST varied according to this decreasing tendency: urban village > residential district > urban park. Urban villages exhibited a warming effect, increasing LST values in buffer zones within 0–150 meters. Conversely, residential districts and urban parks demonstrated cooling effects, decreasing LST values in buffer zones within 0–90 meters and 0–150 meters, respectively. Notably, the cooling effect of urban parks was considerably more pronounced than that of residential districts. Furthermore, the LST of residential districts was influenced by their green coverage, building density, and population. A power function model was observed between green coverage and the inner LST difference within residential districts. LST was also significantly affected by the area, perimeter, and perimeter-to-area ratio of the three land-use types. As area and perimeter increased, the warming effect of urban villages became more apparent, while the cooling effects of residential districts and urban parks were amplified. The LST of urban parks was also affected by their internal ecological land-use types (including forests, water bodies, and grasslands) and landscape characteristics. Stepwise regression analysis indicated cooling effects could be enhanced by reducing landscape fragmentation, simplifying shapes and increasing division level of construction land, as well as increasing water area proportion and water patch aggregation within urban park plan. In conclusion, thermal landscape dynamics are obviously shaped by the degree of interaction between land use patterns and processes in urban area.

Keywords: urban heat island, land surface temperature, urban village, residential district, urban park, landscape pattern.

INTRODUCTION

Recent studies indicate that urbanization and industrialization significantly contribute to urban heat islands (UHIs). UHIs are characterized by higher atmospheric and surface temperatures in urban areas compared to surrounding rural areas (Mas'Uddin et al., 2023; Wang et al., 2024). Typically, UHIs are found in densely populated urban zones with consistently higher energy consumption than adjacent rural regions (Wang and Guan, 2012; Tian et al., 2021). Currently, over half of the global population lives in cities, accounting for over 60% of the world's total energy consumption (Malley et al., 2015; United Nations Human Settlements Programme, 2023). These highly-dense urban areas are often feature a high density of buildings and structures with low thermal capacity but high heat accumulation rate, causing them to absorb more solar radiation (Jamei et al., 2021). The rising atmospheric and surface temperatures, coupled with the presence of UHIs, have had severe and harmful consequences on human health and well-being (Xu, et al., 2017a; Wang et al., 2023). UHIs can also influence local weather and climate through altering local weather and climate patterns (Singh et al., 2017; Luo et al., 2022). As a result, the UHI phenomenon has evolved into one of the vital social and climate-related challenges worldwide.

Land use/cover change (LUCC) has been accelerated by the urbanization process along with population growth and economic expansion (Dadashpoor et al., 2019; Yu et al., 2022). It is widely recognized that urban LUCC can have a certain impact on the thermal environment patterns. This is because different land use/cover types possess distinct characteristic thermal, moisture, and optical spectral properties (Chen and Zhang, 2017; Roy et al., 2022). In recent years, most of studies have utilized remote sensing data, field observation data, and mesoscale models like the weather research and forecasting (WRF) model to assess the ways in which LUCC can modify urban thermal patterns (Kubota et al., 2017; Harmay et al., 2021; Yuan et al., 2023). These studies partially revealed the synergistic reaction mechanism between LUCC and thermal patterns in the process of UHIs. Previous research has verified that in urban areas, both vegetation cover and water bodies are conducive to reducing LST and enhancing the relative humidity of the air. Due to their cooling effects on the urban thermal environment, they have been referred to as "cold islands" (Chapman et al., 2018; Masoudi et al., 2021; Gao et al., 2022). UHI effects mitigated by both vegetation cover and water can be explained as follows: (1) a significant portion of sunlight and environmental radiative waves can be reflected by vegetation and water bodies; (2) thermal energy and air moisture can be readily mediated through water evaporation, vegetation transpiration and vegetation photosynthesis.

It is commonly acknowledged that urban parks are abundant in vegetation and water bodies. As a result, they assume a crucial role in mitigating the urban thermal environment (Peng et al., 2016; Zhu et al., 2023). Many UHI studies have discussed how cooling effects of urban parks could be affected by the geometric forms such as park area, perimeter and ratios between park area and perimeter (Wang, et al., 2017a; Gao et al., 2022; Cai et al., 2023). Some studies focused on how cooling effects of urban parks are affected by inner land-use landscape characteristics of urban parks (Xu, et al., 2017b; Liao et al., 2023). Generally, urban parks are regarded as vital urban public spaces that offer opportunities for natural landscape appreciation, recreational activities, and relaxation. Simultaneously, urban villages and residential districts serve as the primary living environments for urban residents. Urban villages are areas surrounded by cities during rapid urbanization, often overlooked in urban planning. They are usually distributed in the urban built-up areas and characterized by a mixture of urban and rural society (Wei et al., 2024), providing affordable and accessible housing for rural migrants (Zhang et al., 2016). Due to exclusion from urban spatial planning, most urban villages developed chaotically during urbanization (Song and Zenou, 2012; Huang et al., 2023). Owing to the scarcity of cooling elements like vegetation cover and water bodies, combined with their high building and population densities, urban villages are frequently plagued by an inhospitable thermal environment marked by elevated temperatures (Qiu et al., 2017). In contrast to urban villages, residential districts, which are governed by governmental development plans and management, typically feature lower building densities and higher vegetation cover. As a result, the thermal conditions in these districts are likely to differ significantly from those in urban villages. While urban parks have been extensively studied for their thermal-regulating effects, the thermal environments and associated regulatory mechanisms of both urban villages and residential districts remain less understood. This knowledge gap is concerning, given that the thermal quality of both urban villages and residential districts directly impacts the living standards of urban residents.

Considering the aforementioned deficiencies in UHI research, three typical land-use types (e.g. urban village, residential district, and urban park) were selected for an in-depth examination of their thermal characteristics and heat regulation mechanisms in Guangzhou, South China. This study helped enhance the understanding of effective strategies for regulating the UHI effect. It furnished scientific data that can serve as a robust foundation for contemporary urban detailed planning and management, thereby facilitating the creation of more sustainable and thermally-comfortable urban environments. To achieve these objectives, the following approaches were adopted: (1) Analyze the LST disparities among three typical land-use types, namely urban villages, residential districts, and urban parks; (2) Quantify how both the inner and outside LST of urban village, residential district and urban park could be affected by the area, parameter and the ratios between area and parameter of three typical land use types; (3) Examine the correlation between urban planning indicators (such as green coverage, building number and plot ratio) and LST in residential districts; (4) Explore how the cooling effect could be affected by inner land-use landscapes of urban parks.

MATERIALS AND METHODS

Study area

Megalopolis Guangzhou (112°57′~114°3′E, 22°26′~23°56′N) is situated in Pearl River Delta, South China (Figure 1). Guangzhou has a typical subtropical marine monsoon climate, featuring relatively high temperatures throughout the year. Average annual temperature exceeds 22 °C, and average temperature in the hottest month, July, is approximately 28 °C. Overall, Guangzhou's climate is marked by warm and rainy conditions, abundant sunlight, a long summer, and a short frost-free period. As a pivotal gateway city for the reform and opening-up in South China, Guangzhou has scored remarkable and unparalleled achievements in urban development. It has successfully evolved into one of the five National Central Cities in China. However, Guangzhou has been continuously troubled by the high-temperature "scorching" climate. The highest annual air temperature has often remained above 37 °C for an extended period, and as a result, the perceived body temperature has exceeded 40 °C. As the renowned "City of Flowers", Guangzhou has always been committed to the planning and development of urban parks, and these urban parks can, to some extent, alleviate the negative impacts of the UHI effect. During the rapid urban development process, a large number of modern residential districts have been constructed in the urban center of Guangzhou. Nevertheless, many urban villages still remain in the urban central areas. The UHI effect can be significantly alleviated by ecological land-use types like forests, water bodies, and grasslands in the urban central areas. Regrettably, in urban villages where the UHI effect is prominent, such ecological land-use types have largely disappeared.

Remote sensing data

With the advancement of remote sensing (RS) and geographic information system (GIS) technologies, the LST retrieved from remote sensing data has been extensively applied to

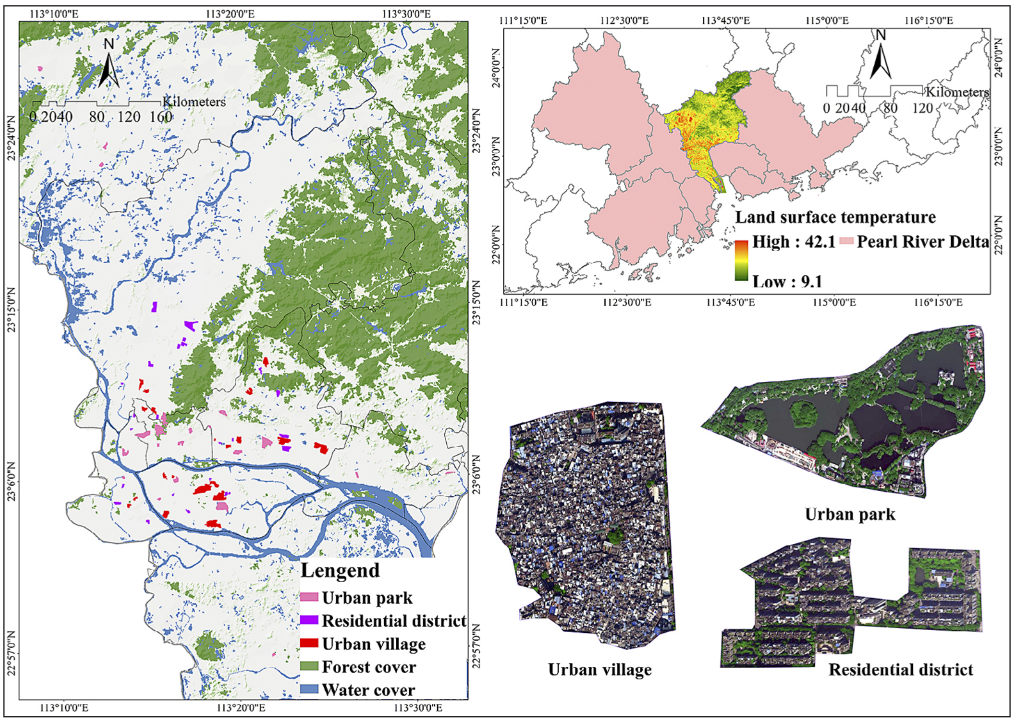

Figure 1. Typical research samples and land surface temperature distribution in Guangzhou

explore how UHI effect can be influenced by various abiotic and biotic factors. In numerous studies, LST can be effectively obtained. In this study, Landsat 8 images featuring multispectral and thermal infrared wavebands were employed to retrieve the LST in Guangzhou. The Landsat 8 images were sourced from the website: http://ids.ceode.ac.cn/. Located in the southern subtropical region, Guangzhou undergoes frequent rainy and cloudy weather, degrading Landsat 8 image quality and resulting in scarce usable imagery for research. Landsat 8 satellite has a typical 16-day revisit cycle. Coupled with the interference of rain, clouds, and fog, its remote sensing imagery struggles to capture short-term or seasonal variation characteristics of the UHI effect. Retrieval results showed that for Landsat 8 images of path 122 and row 44 with cloud cover below 5% in 2014, the acquisitions on January 17, 2014 (1.62% cloud cover), November 16, 2011 (0.56% cloud cover), and October 15, 2014 (0.17% cloud cover) were eligible. However, the first two images exhibited evident cloud interference over the Guangzhou region, leaving only the October 15, 2014 image that met the research criteria. On that day, October 15, 2014, the highest temperature was 30 °C and the lowest temperature was 17 °C. The coordinate system of the selected remote sensing images is the WGS-84. To reduce atmospheric impacts, multispectral images were radiometrically corrected using the FLAASH model in ENVI 5.1 and geometrically corrected with ground control points. Then, the images were clipped by Guangzhou's vector map.

Sampling data for three typical land-use types

To understand how abiotic and biotic factors can effectively regulate the UHI effect of three typical land-use types in Guangzhou, 21 urban parks, 23 urban residential districts, and 17 urban villages were selected from the urban development areas. Owing to the absence of statistical data including population and plot ratio, along with the lack of scientific planning and management, this study merely analyzed the impact of the area, perimeter, and the perimeter-to-area ratio of urban villages on their LST characteristics. Additionally, it analyzed how the area, perimeter, and perimeter-to-area ratio affect the LST characteristics of urban residential districts and urban parks. Meanwhile, this study aimed to explore how the LST characteristics of urban residential districts could be alleviated by planning indicators, including plot ratio, green coverage, building number and household number. This study also analyzed how the LST both inside and outside urban parks would be influenced by the land-use landscape characteristics of urban park, aiming to reveal the thermal regulation mechanisms of these urban parks. The GIS buffer analysis function was employed to extract the average LST of various buffer zones ranging from 0 to 540 meters outside the three typical land-use types. The buffer distance interval was set at 30 meters, in accordance with the spatial resolution of the Landsat data. The buffer zone analysis was conducted to uncover the correlation relationships between the internal and external LST characteristics.

LST extraction

Currently, there are three main LST inversion algorithms: the atmospheric correction method (also known as the radiative transfer equation), the single-channel algorithm, and the split-window algorithm. However, these algorithms differ in their sensitivity to parameters such as atmospheric conditions and surface emissivity, which may introduce errors into LST inversion results. Despite this, Landsat data remains a critical data source for studying the urban heat island effect. When atmospheric parameters and surface emissivity are known or can be accurately estimated, the radiative transfer equation (RTE) enables high-precision retrieval of LST (Xu et al., 2015; Windahl and de Beurs, 2016; Wang et al., 2018). RTE was utilized to retrieve the LST in this study. The main formulas are as follows:

$$L_\lambda = 0.0003342 Q_{DN} + 0.1 \tag{1}$$

$$TB = \frac{K_2}{\ln\left(\frac{K_1}{L_\lambda} + 1\right)} \tag{2}$$

$$LST = \frac{\rho TB}{\rho + \lambda TB \ln \varepsilon} - 273.15 \tag{3}$$

where: L_λ represents the land surface radiation value, Q_{DN} is the grey level value of the tenth thermal infrared band of Landsat 8 images; TB stands for radiant brightness temperature; K_1 and K_2 are default values, with values of 774.89 W•m^{-2}•sr^{-1}•μm^{-1} and 1321.08 K, respectively. λ represents the central wavelength of the tenth thermal infrared band, valuing 10.9 μm. ρ is constant 0.01438 m•K. ε represents surface feature emissivity. The ε calculation method is described in Griend and Owe (1993) and Weng (2003).

Calculation of landscape pattern index

Three typical land use types, namely urban villages, residential districts, and urban parks, were identified based on Baidu Maps and on-site investigations. Their specific locations and spatial areas were meticulously verified with the aid of high-resolution Google Earth images. Additionally, shape characteristics such as area, perimeter, and the ratio between perimeter and area for these land use types were calculated by ArcGIS 10.2 software. In order to investigate the land-use landscape characteristics of urban parks, the various land-use types (such as construction land, forest land, water area, and grassland) of urban parks were retrieved through manual visual interpretation of Google Earth images. The KML files of different land-use types were opened in ArcGIS 10.2 software for topology checking and the conversion of data format from vector to raster. To extract the landscape pattern index, the land-use data of urban parks were transformed into TIF grid formats. The landscape pattern index was calculated using the Fragstats 4.2 software. Since water areas and grasslands do not exist in all urban parks, forest land, water areas, and grasslands were aggregated as ecological land. The landscape pattern index of the ecological land was also retrieved to analyze the thermal regulation functions and mechanisms of the ecological land.

Drawing on previous research on the UHI effect, eight landscape pattern indexes for urban park land use were calculated at the class metrics level in Guangzhou's urban parks. These indexes encompass patch density (PD), largest patch index (LPI), total edge (TE), edge density (ED), mean area (AREA_MN), mean shape index (SHAPE_MN), landscape division index (DIVISION) and aggregation index (AI). Simultaneously, ten landscape indexes were computed at the landscape metrics level for the same urban parks in Guangzhou. This set includes PD, LPI, TE, ED, AREA_MN, DIVISION, patch richness (PR), patch richness density (PRD), Shannon diversity index (SHDI) and AI.

Statistical analyses

Correlation analysis was initially employed to identify the parameter that could have an impact on the LST. Subsequently, linear, logarithmic, power, and exponential functions were utilized to analyze the differential correlations between the minimum, average, and maximum LST values and the area, perimeter, as well as the perimeter-to-area ratio of each typical land-use type in Guangzhou. Statistical analyses were predominantly conducted using SPSS 19.0 and Origin 9.0 at a 95% confidence level. The key statistical methods employed included correlation analysis, linear regression analysis, nonlinear regression analysis, and stepwise regression analysis. Correlation and stepwise regression analyses were executed via SPSS 19.0, whereas linear and nonlinear regression analyses, along with the generation of their corresponding graphical plots, were accomplished using Origin 9.0.

RESULT AND DISCUSSION

LST differences among three typical land-use types

Generally, the LST values of urban villages, residential districts, and urban parks differed significantly, and their influence ranges on the surrounding thermal environment also varied distinctly (Figure 2). The results demonstrated that the minimum, average, and maximum LST values all exhibited a decreasing trend in the following order: urban village > residential district > urban park. The average LST of urban villages, residential districts, and urban parks were 28.59 °C, 26.95 °C, and 25.09 °C, respectively. Cao et al. (2022) reported a similar finding: in Wuhan of China, high-density residential areas exhibit higher temperatures and drier conditions than low-density residential areas with scattered layouts and extensive open spaces. Kolokotsa et al. (2022) found that in the Sydney Metropolitan Area, higher built area ratio of precincts correlated with lower cooling contribution of mitigation measures. LST variations among three typical land-use types can be explained by large differences in ecological land-use types. Firstly, notable disparities exist in vegetation cover among the three typical land-use types. In Guangzhou, urban villages are characterized by a scarcity of ecological land cover, including forest cover, water bodies, and grasslands. In contrast, residential districts feature a green coverage rate ranging from 17% to 50%. Urban parks stand out prominently, with their ecological land cover exceeding 72%. In some cases in Guangzhou, the ecological land cover within urban parks can even reach as high as 97.62%. Previous studies have predominantly shown that ecological land cover can alleviate thermal conditions via cooling and humidifying effects. A vast majority of these studies have indicated that LST is negatively correlated with vegetation cover, forest cover, water area ratio, and ecological land cover (Peng et al., 2016; Masoudi et al., 2021; Zhu et al., 2023). In addition, urban villages are almost entirely covered by artificial buildings. They are characterized by high population density, a large number of densely-packed artificial buildings, crowded streets and roads, and a lack of ventilated cooling channels (Zhang and Meng, 2013; Guo et al., 2015). Thus, the urban village exhibited the highest LST.

Buffer zone analysis showed that due to their heat island effects, urban villages significantly warmed the surrounding thermal environment. This warming was mainly confined to the 0–150 m buffer zones; beyond this distance, the warming effects of urban villages dissipated. The maximum LST difference between urban villages and their surrounding buffer zones was 0.83 °C. Unlike urban villages, residential districts and urban parks cooled the surrounding areas. Aram et al. (2019) found that a 125-hectare urban park in Madrid, Spain, reduced air temperatures by an average of 0.63 °C at a distance of 150 meters from the park, with the cooling effect decreasing to 1.28°C at distances of 380 meters and 665 meters. A study by Zhang et al. (2024) on 33 urban parks in Harbin, China, revealed that the parks had an average cooling range of 277 meters and achieved an average cooling effect of 3.27 °C. In Guangzhou, average cooling ranges of residential districts and urban parks are 90 m and 150 m, respectively, both decreasing with the increasing buffer distance. The maximum LST differences were 0.67 °C for residential districts and 2.45 °C for urban parks compared to their buffer zones. In conclusion, urban parks have a more pronounced cooling effect than residential districts. Regression analysis indicated that in

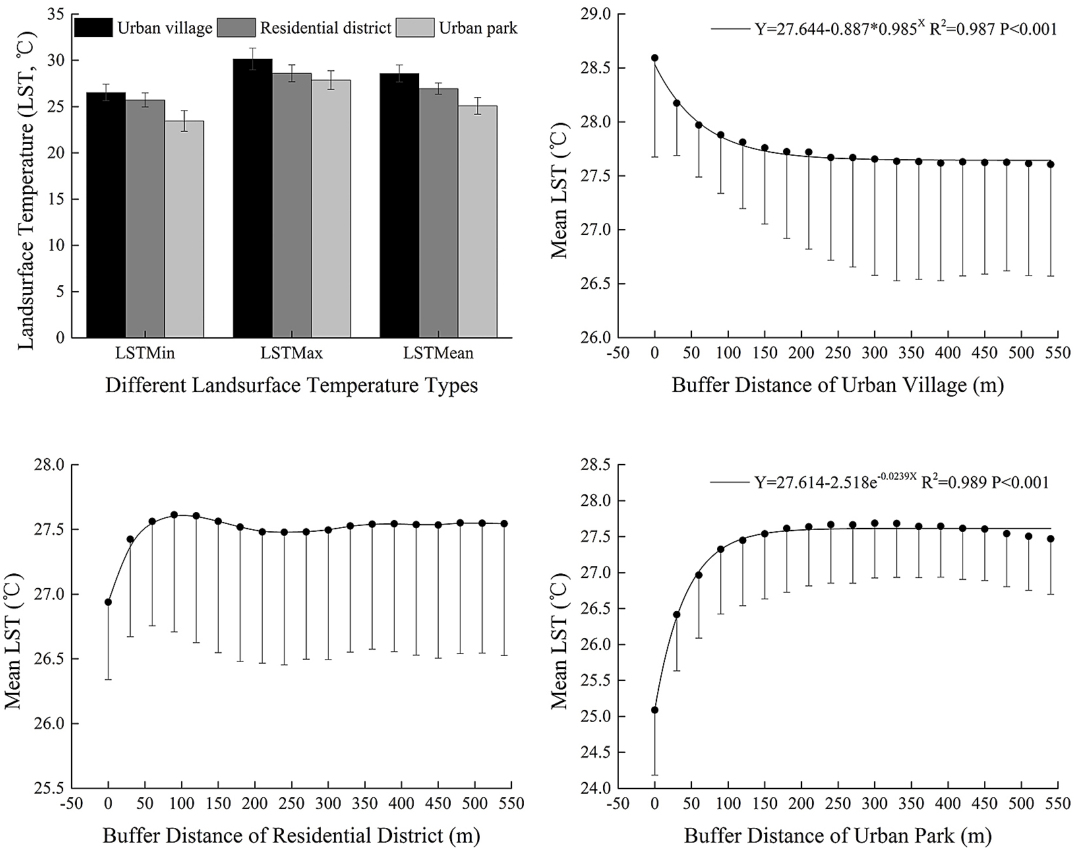

Figure 2. LST differences among three typical land-use types in Guangzhou

both urban villages and urban parks, there were robust power- function relationships between LST and buffer distance, with determination coefficients (R^2) exceeding 0.98. Conversely, no such fitting function relationship was established between LST and buffer distance in residential districts (Figure 2).

LST variations affected by basic characteristics of three typical land-use types

Recent studies mainly examined how an urban park's area, perimeter, and ratio between perimeter and area affect LST, but few have investigated urban residential districts and urban villages. Previous studies showed that the area and perimeter of urban parks were negatively correlated with LST, whereas the ratio between perimeter and area was positively correlated with LST (Liu et al., 2017; Algretawee, 2022; Cai et al., 2023; Liao et al., 2023). Moreover, the area, perimeter, and ratio between perimeter and area of urban parks did not exhibit simple linear correlations with LST. Instead, they were correlated with LST following exponential, logarithmic, and power functions, respectively. This study corroborated the conclusions of previous research (Meng et al., 2010; Li and Pan, 2017). As shown in Table 1, the maximum LST was positively correlated with the area and perimeter of urban villages while it was negatively correlated with the ratio between perimeter and area. This result can be attributed to several factors. In urban villages of Guangzhou, there is a high building density and a large contiguous building distribution area (Zhang et al., 2016; Zhou and Chen, 2018; Wei et al., 2024). Additionally, the absence of cooling corridors in these urban villages makes it difficult for thermal exchange to occur between the interior of the urban villages and the outside environment (Guo et al., 2015). A higher ratio between perimeter and area implies greater shape complexity of land use patches, which promotes energy flow, matter cycling, and information exchange between urban village interiors and exteriors. As this ratio rises, more frequent energy exchanges help reduce internal LST differences. There was a significant power-function correlation relationship between the LST and the ratio between perimeter and area of urban villages in Guangzhou (R^2 = 0.615, Figure 3).

Unlike urban villages, residential districts showed distinct relationships between LST and geometric characteristics, as presented in Table 1. Specifically, both the minimum and average LST values of residential districts were negatively correlated with their area and perimeter. Conversely, these LST values were positively correlated with the inner LST difference within the residential districts. Additionally, the inner LST difference of residential districts exhibited a negative correlation with the ratio of perimeter to area. Regression analysis revealed a significant power-function relationship between the inner LST difference and the perimeter- to- area ratio of residential districts (R^2 = 0.456, Figure 4). These results showed that in urban residential districts, scientific building plans to increase area and perimeter can lower LST. Larger areas and perimeters enhance energy exchange between the inside and outside of districts, directly reducing the minimum LST and inner LST difference. Moreover, larger residential districts with greater perimeters mean more ecological land, helping to lower internal LST. Additionally, the inner LST difference decreases as the ratio between perimeter and area of residential districts increases. For residential districts in high UHI-effect areas, this suggests appropriately decreasing the perimeter-to-area ratio to limit energy exchange

Table 1. Correlational relationship between LST and perimeter, area and ratio between perimeter and area of three typical land-use types in Guangzhou

Factor	Urban village			Residential district			Urban park		
	Perimeter	Area	RPA	Perimeter	Area	RPA	Perimeter	Area	RPA
LST_{Min}	-0.347	-0.349	0.378	**-0.559****	**-0.610****	0.366	-0.315	**-0.541***	**0.560****
LST_{Max}	**0.657****	**0.669****	-0.298	0.196	0.230	-0.283	-0.173	-0.146	-0.091
LST_{Mean}	0.084	0.076	0.041	**-0.414***	**-0.440***	0.213	**-0.747****	**-0.697****	**0.578****
LST_D	**0.837****	**0.849****	**-0.534***	**0.566****	**0.631****	**-0.503***	0.156	0.363	**-0.529***

Note: $^{**}P < 0.01$; $^{*}P < 0.05$; LST_{Min}, LST_{Max} and LST_{Mean} signify the minimum, maximum and average LST of each urban land-use types, respectively; LST_D stands for the inner LST difference of each urban land-use types; RPA stands for ratio between perimeter and area of each typical land-use type.

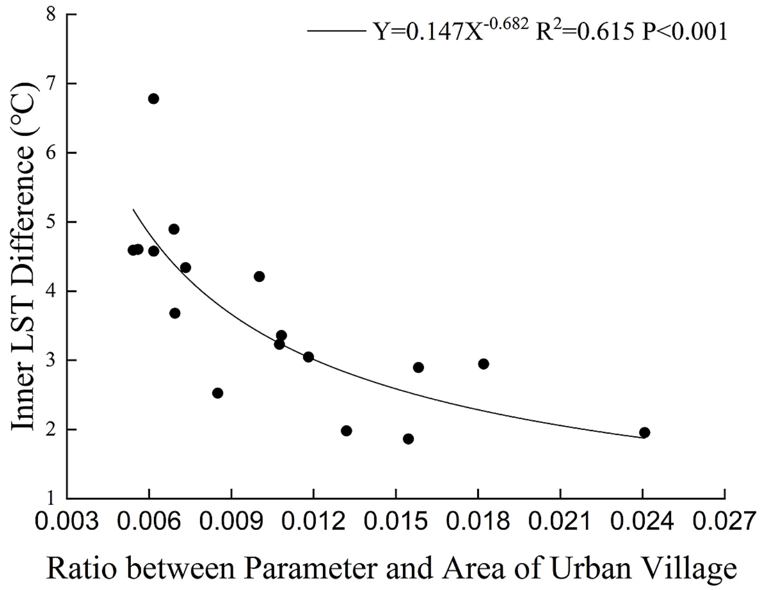

Figure 3. Correlation relationship between inner LST difference and ratio between perimeter and area of urban villages in Guangzhou

and manage LST. Furthermore, correlation analysis results showed that the thermal environment of residential districts could be mitigated by a change in green coverage, building number and household number (Table 2). It is widely recognized that green coverage is a crucial ecological factor influencing the thermal environment of residential districts (Yue and Xue, 2016; Zhu et al., 2023). Liao et al. (2021) reported that within residential districts in Changsha, China, trees exhibit the most pronounced cooling effect with superior vertical cooling performance, followed by shrubs, while grassland shows the least effective cooling. To enhance thermal environmental comfort, the cooling effects of both green coverage and its shading attributes should be comprehensively considered (Liao et al., 2021). Zheng et al. (2024) revealed in Changsha that increasing the green plot ratio (GPR) in residential districts can effectively mitigate UHI intensity and enhance thermal comfort. When the GPR reaches 3.5, all four types of spaces exhibit “moderate” UHI intensity. This study further revealed that in Guangzhou, southern China, green coverage positively correlated with both the minimum and average LST. Additionally, there exists a quadratic function fitting relationship between the inner LST difference and green coverage (R^2 = 0.365, Figure 4). The findings suggested that augmenting green coverage could, to some extent, ameliorate the thermal environment of residential districts. Yet, Figure 4 revealed a nuanced relationship: when green coverage was below 30%, the inner LST difference diminished as greenery expanded; conversely, once green coverage surpassed 30%, the inner LST difference escalated with additional greening. This dichotomy stemmed from the cooling mechanisms of green spaces. When green coverage was below 30%, more greenery significantly boosted ventilated cooling efficiency. But once it exceeded 30%, this efficiency no longer increased linearly. Meanwhile, as green coverage grew, the energy exchange efficiency between inner construction and green areas in residential districts decreased, leading to the rise in the inner LST difference. In addition, correlation analysis revealed that both the maximum LST and the inner LST difference of residential districts were positively correlated with the building number (Table 2). This indicates that an increase in building number would deteriorate the thermal comfort conditions. The analysis found that the minimum LST was negatively correlated with the household number, whereas the inner LST difference was positively correlated with it. However, this does not imply that an increase in household number would directly lead to a decrease in the minimum LST and the inner LST difference within residential districts. Notably, the household number was strongly positively correlated with the area and perimeter of residential districts (R > 0.7). Consequently, the expansion of green coverage accompanying the growth in the number of households could lower

Table 2. Correlational relationship between LST and other parameters of both residential district and urban park in Guangzhou

Factor	Residential district				Urban park		
	Plot ratio	Green coverage	Building number	Household number	Forest land	Ecological land	Construction land
LST_{Min}	0.126	**-0.608****	-0.307	**-0.425***	-0.302	**-0.527***	**-0.456***
LST_{Max}	-0.261	-0.084	**0.460***	0.337	-0.146	-0.157	-0.045
LST_{Mean}	0.036	**-0.637****	-0.114	-0.255	**-0.750****	**-0.708****	**-0.443***
LST_{D}	-0.314	0.359	**0.613****	**0.591****	0.161	0.344	0.355

Note: $^{**}P < 0.01$; $^{*}P < 0.05$; LST_{Min}, LST_{Max} and LST_{Mean} signify the minimum, maximum and average LST of each urban land-use types, respectively; LST_D stands for the inner LST difference of each urban land-use types.

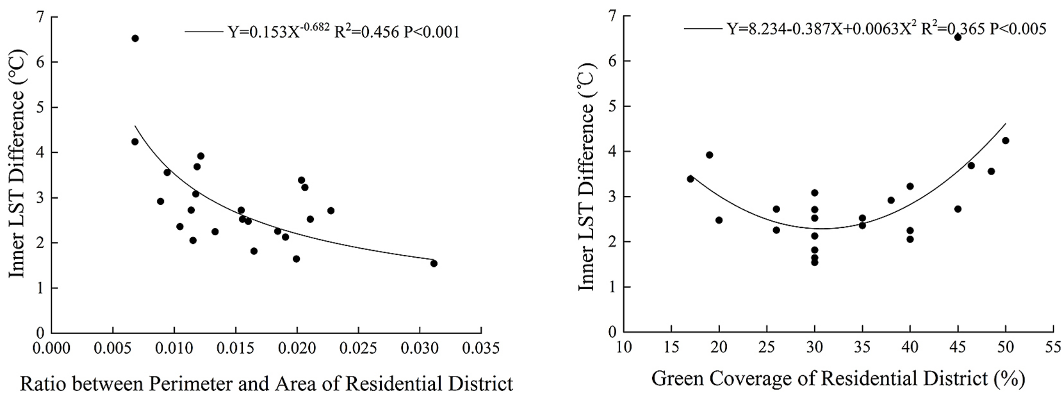

Figure 4. Correlation relationships between ratio between perimeter and area, green coverage and inner LST difference of residential districts

the minimum LST, which in turn would increase the inner LST difference of residential districts. Like residential districts, urban parks' average LST correlated negatively with perimeter and area, while minimum LST correlated negatively with area (Table 2). Increasing the perimeter and area of urban parks significantly reduced their average and minimum LST values, enhancing the parks' cooling effect. Further, Figure 5 showed power function relationships between the mean LST and urban park area ($R^2 = 0.588$), as well as between the mean LST and perimeter ($R^2 = 0.549$). A power function relationship between the minimum LST and perimeter was also detected in urban parks ($R^2 = 0.262$). Meanwhile, Table 2 revealed that the perimeter-to-area ratio had a significant positive correlation with both the minimum and average LST of urban parks. Additionally, a power function fitting relationship existed between the minimum LST and the perimeter-to-area ratio ($R^2 = 0.397$). These results indicated that as the ratio between perimeter and area increased, the more complex boundaries of urban parks facilitated energy exchange between the internal and external environments. Frequent energy exchange between the inner and outside environment would raise the minimum LST, which would subsequently lead to an increase in the average LST. Correlation analysis further showed that thermal environment of urban parks was affected by internal land-use types. Average and minimum LSTs negatively correlated with ecological and construction land areas, and average LST also negatively correlated with forest land area (Table 2). Ecological land cover could mitigate LST through vegetation photosynthesis, transpiration, evapotranspiration and water evaporation, etc. Figure 5 showed significant power function relationships between LSTs and forest, water, and ecological land areas. Zou et al. (2021) found that in Shenzhen, South China, a 10% increase in natural underlying surface coverage—including woodland, lawn, water bodies, and bare land—led to a 0.38–0.39 °C decrease in nighttime UHI intensity. It was indicated that ecological land-use adjustment would be effective in mitigating urban parks' LST. However, urban parks' cooling effect efficiency would be in a decreasing trend as ecological land area increased (Figure 5).

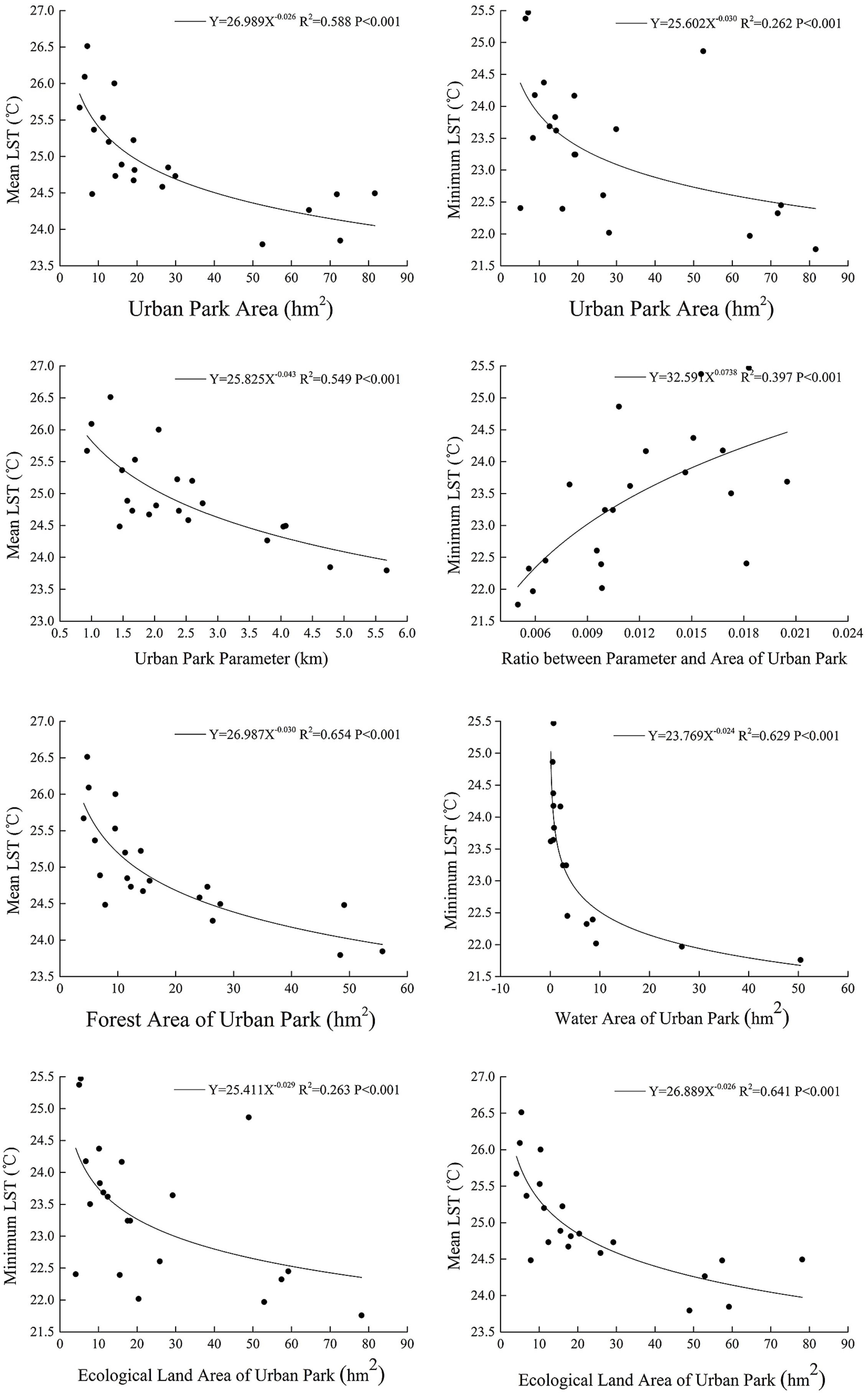

Figure 5. Correlation relationships between LST and parameters of urban parks in Guangzhou

Cooling effects affected by landscape patterns of inner-urban parks

In urban developing areas, thermal landscape dynamics are significantly determined by the extent of interaction between land use patterns and related processes (Silva et al., 2018; Nastran et al., 2019; Cai et al., 2023; Liao et al., 2023). Most studies focused on the impact of land-use landscapes on urban LST. They have revealed that urban land-use patterns exert a crucial influence on the UHI effect at a regional level (Wang and Guan, 2012; Wang, et al., 2017b; Liu et al., 2024). However, few studies have delved into the influence of internal land-use pattern of urban parks on LST. Hence, this study aims to explore how the internal land-use landscape of urban parks in Guangzhou impacts LST, considering both class-level and landscape-level metrics (Table 3). From the perspective of landscape metrics, landscape pattern indices such as PD, TE, and PDR were significantly correlated with the minimum LST, average LST, and the inner LST difference of urban parks. AREA_MN was negatively correlated with the minimum LST and average LST. ED and AI were significantly correlated with the average LST, while PR was positively correlated with the inner LST difference of urban parks. In particular, PD was employed to depict the land-use patch fragmentation, ED was utilized to illustrate the landscape heterogeneity, PRD was used to characterize patch abundance and density. Moreover, PD, ED, and PRD all exhibited a positive correlation with the mean LST. PD and PRD were also positively correlated with the minimum LST but negatively correlated with the inner LST difference. The increase in PD, ED, and PRD led to an elevation in LST and a reduction in the cooling effect of urban parks. In other words, the cooling capabilities of urban parks would be diminished, and the average LST of urban parks would rise when land-use fragmentation, patch density, and landscape heterogeneity increased within urban parks. Gao et al. (2023) similarly found in a study of 36 urban parks in Zhengzhou, Central China, that green space ED and PD within parks showed significant negative correlations with cooling effect indicators. However, in Zhengzhou, Cai et al. (2023) found that perimeter, area, internal green coverage, and landscape shape index of urban parks were the primary factors correlated with maintaining a low LST in urban parks. Furthermore, TE represented the total edge length, AREA_MN indicated the average landscape patch area, and AI reflected the landscape patch aggregation. TE, AREA_MN, and AI were all negatively correlated with the mean LST. Meanwhile, both TE and AREA_MN, which were correlated with each other, were negatively correlated with the minimum LST, and TE was positively correlated with the inner LST difference. These results implied that an increase in the landscape patch area and the patch aggregation level could significantly reduce the LST, thereby enhancing the cooling effects of urban parks.

Correlation analysis results also demonstrated that urban park's LST was regulated by the landscape patterns of different internal land-use types at a class metric level (Table 4). Both PD and ED of ecological land were positively correlated with mean LST. Additionally, ED of ecological land was positively correlated with the minimum LST and negatively correlated with the inner LST difference. This result indicated that in urban parks, when patch fragmentation and edge density increased, the processes of energy flow, material cycle, and information exchange between ecological patches and the surrounding construction patches would become more efficient, leading to an increase in LST of ecological land. Both LPI and AREA_MN of ecological land negatively correlated with mean LST. AREA_MN of

Table 3. Correlational relationship between LST and landscape indexes of urban-park land use at the landscape metrics in Guangzhou

Factor	PD	LPI	TE	ED	AREA_MN	DIVISION	PR	PRD	SHDI	AI
LST_{Min}	**0.673****	0.28	**-0.686****	0.373	**-0.589****	-0.195	-0.373	**0.887****	-0.261	-0.418
LST_{Max}	0.157	-0.178	-0.107	-0.007	-0.213	0.204	0.326	0.087	0.214	0.016
LST_{Mean}	**0.646****	-0.145	**-0.552****	**0.442***	**-0.438***	0.210	-0.311	**0.825****	0.121	**-0.469***
LST_D	**-0.466***	-0.35	**0.509***	-0.319	0.36	0.294	**0.522***	**-0.691****	0.356	0.362

Note: $^{**}P < 0.01$; $^{*}P < 0.05$; LST_{Min}, LST_{Max} and LST_{Mean} signify the minimum, maximum and average LST of each urban land-use types, respectively; LST_D stands for the inner LST difference of each urban land-use types.

ecological land also negatively correlated with the minimum LST but positively with inner the LST difference. This result indicated that larger ecological land patches could partially reduce energy exchange with the surroundings, thereby decreasing ecological land LST and enhancing urban parks' cooling effects. Table 4 indicated that AI of ecological land had a negative correlation with both the mean and minimum LST, and a positive correlation with the inner LST difference. Meanwhile, DIVISION of ecological land was positively correlated with mean LST. This implied that the cooling effect of urban parks could be enhanced as the aggregation level of ecological land increased. Since ecological land in urban parks was mainly composed of forest land, these correlation relationships between LST and landscape indexes of forest land were similar to that of ecological land in urban parks (Table 4). However, both DIVISION and AI were not significantly correlated with LST, while TE was significantly correlated with the minimum LST, average LST and inner LST difference. Moreover, the proportion of ecological land exhibits a negative correlation with mean LST, whereas the proportion of forest land shows a positive correlation with the minimum LST. This phenomenon can be attributed to the fact that in Guangzhou, when these selected urban parks are smaller, the proportion of forest land is relatively higher, and these smaller urban parks are more susceptible to the surrounding thermal conditions. Consequently, the proportion of forest land was positively associated with the minimum LST.

Evidently, the minimum LST of water area is negatively correlated with both TE and AREA_MN, while it is positively correlated with DIVISION. In other words, when water area expands, edge length increases, and the distance between water patches shortens, the minimum LST of urban parks will significantly decline, mainly because water has the highest heat capacity among the different internal land-use types of urban parks. Additionally, it has been found that water area proportion in urban parks in Guangzhou was also negatively correlated with the minimum LST (Table 4). Compared with the cooling effects exerted by the ecological land, forest land, and water area within urban parks, construction land in urban parks shows obvious warming effects (Table 4). This could be underlined as follows: (1) The construction land proportion was positively correlated with average LST; (2) Both PD and ED of construction land were positively correlated with the minimum LST and average LST, but negatively correlated with the inner LST difference; (3) LPI was positively correlated with average LST, while DIVISION was positively correlated with the maximum LST and average LST, and AI has a significant positive correlation with the inner LST difference. These results indicated that when the patch fragmentation of construction land increased, along with an increase in the maximum patch area and a decrease in the distance between construction land patches, LST of urban parks would tend to rise, and their cooling effects would weaken.

Decisive landscape indexes correlated with urban parks' LST

As Table 4 shows, landscape indexes' correlations with urban park LST are complex and variable. Thus, stepwise regression analysis was conducted to identify the decisive factors. The results of these models are presented in Table 5. It can be seen from Table 5 that these influence degrees of different decisive landscape indexes on the minimum LST of urban parks were: PRD at a landscape metric > water area ratio > PD of construction land. A higher PRD partly implies a greater fragmentation of landscape patches in urban parks. This finding suggests that a higher PRD, a smaller proportion of the water area, and a higher density of construction patches will lead to a higher minimum LST in urban parks. At the same time, these influence degrees of different decisive landscape indexes on the maximum LST of urban parks were as follows: DIVISION of construction land > SHAPE_MN of construction land > PD of water area. This result indicated that a lower patch fragmentation of construction land, a more intricate morphological structure of construction land, and a higher patch density of water area would give rise to a higher maximum LST in urban parks. In other words, construction land with high aggregation and morphological structures is unable to contribute to the LST reduction in urban parks. The decisive influencing factors of average LST in urban parks were shown as PRD at a landscape metric > DIVISION of construction land. This result suggests that greater landscape patch fragmentation, along with a shorter distance between construction land patches, will lead to a higher average LST in urban parks. In contrast with the minimum LST, mean LST and maximum LST, the inner LST difference of urban

Table 4. Correlational relationship between LST and landscape indexes of urban-park land use at the class metrics in Guangzhou

Land use type	LST	Land use cover (%)	PD	LPI	TE	ED	AREA_MN	DIVISION	AI
Forest land	LST_{Min}	**0.437****	**0.615******	0.327	**-0.678******	**0.446****	**-0.497****	-0.286	-0.184
	LST_{Max}	-0.061	0.133	-0.189	-0.134	-0.039	-0.159	0.204	-0.064
	LST_{Mean}	0.005	**0.676******	-0.117	**-0.577******	**0.460****	**-0.681******	0.153	-0.417
	LST_D	-0.406	-0.432	-0.396	**0.485****	-0.401	0.317	0.371	0.114
Water area	LST_{Min}	**-0.593****	0.371	-0.467	**-0.717******	-0.204	**-0.541****	**0.514****	-0.426
	LST_{Max}	-0.274	0.400	-0.330	-0.291	-0.122	-0.342	0.255	-0.276
	LST_{Mean}	-0.167	0.468	-0.124	-0.407	0.129	-0.305	0.186	-0.180
	LST_D	0.372	-0.056	0.204	0.476	0.105	0.266	-0.306	0.205
Construction land	LST_{Min}	0.342	**0.645******	0.344	-0.393	**0.720******	-0.336	-0.288	-0.359
	LST_{Max}	0.216	0.023	0.364	-0.057	-0.057	0.070	**-0.453****	0.301
	LST_{Mean}	**0.496****	**0.482****	**0.579******	-0.430	**0.607******	-0.083	**-0.560****	0.002
	LST_D	-0.15	**-0.529****	-0.058	0.296	**-0.643******	0.327	-0.047	**0.497****
Ecological land	LST_{Min}	-0.342	**0.667******	-0.293	-0.393	**0.720******	**-0.707******	0.341	**-0.743******
	LST_{Max}	-0.216	-0.059	-0.323	-0.057	-0.057	-0.192	0.284	-0.044
	LST_{Mean}	**-0.496****	**0.631******	**-0.483****	-0.430	**0.607******	**-0.701******	**0.524****	**-0.663******
	LST_D	0.150	**-0.599******	0.041	0.296	**-0.643******	**0.473****	-0.106	**0.597******

Note: $^{**}P < 0.01$; $^{*}P < 0.05$; LST_{Min}, LST_{Max} and LST_{Mean} signify the minimum, maximum and average LST of each urban land-use types, respectively; LST_D stands for the inner LST difference of each urban land-use types.

parks were only determined by PRD at a landscape metric (Table 5). As stated above, LST of urban parks and their associated cooling effects are significantly influenced by the landscape patch fragmentation, the morphological structure and patch fragmentation of construction land, as well as the proportion of water area and its corresponding patch fragmentation.

Table 5. Stepwise regression models between LST and landscape pattern indexes of urban park in Guangzhou

Predicted dependent variable	Predicted model	Predicted variable	Standardized coefficients	Determination coefficient R^2
LST_{Min}	Model I	PRD[a]	0.879	0.772
	Model II	PRD[a]	0.768	0.882
		Percent of water area	-0.349	
	Model III	PRD[a]	0.617	0.916
		Percent of water area	-0.501	
		PD[b]	-0.256	
LST_{Max}	Model I	DIVISION[b]	-0.518	0.268
	Model II	DIVISION[b]	-0.824	0.508
		SHAPE_MN[b]	-0.577	
	Model III	DIVISION[b]	-0.809	0.656
		SHAPE_MN[b]	-0.589	
		PD[c]	0.385	
LST_{Mean}	Model I	PRD[a]	0.853	0.728
	Model II	PRD[a]	0.759	0.844
		DIVISION[b]	-0.354	
LST_D	Model I	PRD[a]	-0.579	0.335

Note: *superscript lower-case letter a indicate that landscape indexes are calculated at landscape metrics; Superscript lower-case letter b and c signify landscape indexes of construction land and water area at class metrics, respectively.

CONCLUSIONS

Investigating ecological approaches to mitigate the UHI effect has become a crucial area of research. In this study, urban villages, residential districts and urban parks in Guangzhou were selected to analyze their differences in thermal characteristics and regulation mechanisms. The result showed that the minimum, maximum and average LST values were accordance with the decreasing tendency: urban village > residential district > urban park. Urban villages exhibit a noticeable warming effect, leading to an increase in the surrounding LST. On the other hand, both residential districts and urban parks demonstrate cooling effects, helping to reduce the ambient LST. LST characteristics of three typical land-use types were unevenly influenced by the perimeter, area, and the ratio of perimeter to area of each typical land type. LST typically had a nonlinear correlation with perimeter, area, and the perimeter-to-area ratio. When the perimeter and area increased while the perimeter-to-area ratio decreased, UHI effect was exacerbated, and the internal LST difference increased in urban villages. LST of residential districts was significantly affected by the green coverage, building number, and household number. Green coverage was a key ecological factor influencing the LST, and there was a power function relationship between the LST and the green coverage in residential districts. These factors that affected the LST of urban parks were complex and changeable. Among these factors, the area and proportion of ecological land (such as forest land, water area and grassland) had an important influence on the LST of urban parks. Urban parks' inner land-use landscape also affected LST. Stepwise regression analysis showed that these key factors affecting LST include PRD at a landscape metric, DIVISION and SHAPE_MN of construction land, PD of water area and water area ratio. Cooling effects of urban parks could be significantly influenced by the landscape fragmentation, the morphological structure and patch fragmentation of construction land, as well as the proportion of the water area and its patch fragmentation.

Acknowledgements

Our work was funded by the Natural Science Foundation of Guangdong, China (No. 2021A1515011574), Science and Technology Program of Guangzhou, China (No. 201707010142) and National Natural Science Foundation of China (No. 41371109).

REFERENCES

1. Algretawee, H. (2022). The effect of graduated urban park size on park cooling island and distance relative to land surface temperature LST. *Urban Climate, 45*, 101255.
2. Aram, F., Solgi, E., García, E.H., Mosavi, A., Várkonyi-Kóczy, A.R. (2019). The cooling effect of large-scale urban parks on surrounding area thermal comfort. *Energies, 12*, 3904.
3. Cai, X.Y., Yang, J., Zhang, Y.Q., Xiao, X.M., Xia, J.H. (2023). Cooling island effect in urban parks from the perspective of internal park landscape. *Humanities & Social Sciences Communications, 101*, 674.
4. Cao, Q., Huang, H., Hong, Y., Huang, X., Wang, S., Wang, L., Wang, L. (2022). Modeling intra-urban differences in thermal environments and heat stress based on local climate zones in central Wuhan. *Building and Environment, 225*, 109625.
5. Chapman, S., Thatcher, M., Salazar, A., Watson, J.E.M., Mcalpine, C.A. (2018). The effect of urban density and vegetation cover on the heat island of a subtropical city. *Journal of Applied Meteorology and Climatology, 5711*, 2531–2550.
6. Chen, X., Zhang, Y. (2017). Impacts of urban surface characteristics on spatiotemporal pattern of land surface temperature in Kunming of China. *Sustainable Cities and Society, 32*, 87–99.
7. Dadashpoor, H., Azizi, P., Moghadasi, M. (2019). Land use change, urbanization, and change in landscape pattern in a metropolitan area. *Science of the Total Environment, 655*, 707–719.
8. Doick, K.J., Peace, A., Hutchings, T.R. (2014). The role of one large greenspace in mitigating London's nocturnal urban heat island. *Science of The Total Environment, 493*, 662–671.
9. Gao, Z., Zaitchik, B.F., Hou, Y., Chen, W.P. (2022). Toward park design optimization to mitigate the urban heat Island: Assessment of the cooling effect in five US cities. *Sustainable Cities and Society, 81*, 103870.
10. Griend, A.A.V.D., Owe, M. (1993). On the relationship between thermal emissivity and the normalized difference vegetation index for natural surfaces. *International Journal of Remote Sensing, 146*, 1119–1131.
11. Guo, Q., Zou, Z., Li, H., Qiu, G. (2015). Analysis on the thermal environment of urban village in Shenzhen. *Ecology and Environmental Sciences, 2403*, 427–435.
12. Harmay, N., Kim, D., Choi, M. (2021). Urban heat island associated with land use/land cover and climate variations in Melbourne, Australia. *Sustainable*

Cities and Society, 69, 102861.

13. Huang, Y.J., Zhang, F., Gao, Y., Tu, W., Duarte, F., Ratti, C., Guo, D.S., Liu, Y. (2023). Comprehensive urban space representation with varying numbers of street-level images. *Computers Environment and Urban Systems, 106*, 102043.
14. Jamei, E., Chau, H.W., Seyedmahmoudian, M., Stojcevski, A. (2021). Review on the cooling potential of green roofs in different climates. *Science of the Total Environment, 791*, 148407.
15. Kikon, N., Singh, P., Singh, S.K., Vyas, A. (2016). Assessment of urban heat islands UHI of Noida City, India using multi-temporal satellite data. *Sustainable Cities and Society, 22*, 19–28.
16. Kolokotsa, D., Lilli, K., Gobakis, K., Mavrigiannaki, A., Haddad, S., Garshasbi, S., Mohajer, H., Paolini, R., Vasilakopoulou, K., Bartesaghi, C., Prasad, D., Santamouris, M. (2022). Analyzing the impact of urban planning and building typologies in urban heat island mitigation. *Buildings, 12*(5).
17. Kong, F., Yin, H., James, P., Hutyra, L.R., He, H.S. (2014). Effects of spatial pattern of greenspace on urban cooling in a large metropolitan area of eastern China. *Landscape and Urban Planning, 128*, 35–47.
18. Kubota, T., Lee, H.S., Trihamdani, A.R., Phuong, T.T.T., Tanaka, T., Matsuo, K. (2017). Impacts of land use changes from the Hanoi Master Plan 2030 on urban heat islands: Part 1. Cooling effects of proposed green strategies. *Sustainable Cities and Society, 32*, 295–317.
19. Li, J., Wang, X., Wang, X., Ma, W., Zhang, H. (2009). Remote sensing evaluation of urban heat island and its spatial pattern of the Shanghai metropolitan area, China. *Ecological Complexity, 6*, 413–420.
20. Li, Y., Pan, J. (2017). Spatial-temporal pattern of thermal environment and cooling effect of parks in summer of Xi'an. *Environmental Science & Technology, 403*, 15–26.
21. Liao, J.J., Tan, X., Li, J.Y. (2021). Evaluating the vertical cooling performances of urban vegetation scenarios in a residential environment. *Journal of Building Engineering, 39*, 102313.
22. Liao, W., Guldmann, J.M., Hu, L., Cao, Q.W., Gan, D.X., Li, X.M. (2023). Linking urban park cool island effects to the landscape patterns inside and outside the park: A simultaneous equation modeling approach. *Landscape and Urban Planning, 232*.
23. Liu, F.F., Yan, W.J., Kong, F.H., Yin, H.W., Ban, Y.L., Wen-Bin, X.U. (2017). A review on the urban green space cooling effect based on field measurement of air temperature. *Chinese Journal of Applied Ecology, 284*, 1387–1396.
24. Liu, Y., An, Z.H., Ming, Y.J. (2024). Simulating influences of land use/land cover composition and configuration on urban heat island using machine learning. *Sustainable Cities and Society, 108*, 105482.
25. Luo, Z.R., Liu, J.H., Shao, W.W., Zhou, J.J., Jia, R.T. (2022). Distribution of dry and wet islands in the Pearl River Delta urban agglomeration using numerical simulations. *Atmospheric Research, 273*, 106170.
26. Masoudi, M., Tan, P.Y., Fadaei, M. (2021). The effects of land use on spatial pattern of urban green spaces and their cooling ability. *Urban Climate, 35*, 100743.
27. Mas'Uddin, Karlinasari, L., Pertiwi, S., Erizal. (2023). Urban heat island index change detection based on land surface temperature, normalized difference vegetation index, normalized difference built-up index: a case study. *Journal of Ecological Engineering, 2411*, 91–107.
28. Meng, D., Xiaojuan, L.I., Gong, H. (2010). The thermal environment landscape pattern and typical urban landscapes effect linked with thermal environment in Beijing. *Acta Ecologica Sinica, 3013*, 3491–3500.
29. Mirzaei, P.A. (2015). Recent challenges in modeling of urban heat island. *Sustainable Cities and Society, 19*, 200–206.
30. Nastran, M., Kobal, M., Eler, K. (2019). Urban heat islands in relation to green land use in European cities. *Urban Forestry & Urban Greening, 37*, 33–41.
31. O'Malley, C., Piroozfar, P., Farr, E.R.P., Pomponi, F. (2015). Urban heat island UHI mitigating strategies: A case-based comparative analysis. *Sustainable Cities and Society, 19*, 222–235.
32. Peng, J., Xie, P., Liu, Y., Ma, J. (2016). Urban thermal environment dynamics and associated landscape pattern factors: A case study in the Beijing metropolitan region. *Remote Sensing of Environment, 173*, 145–155.
33. Qiu, G.Y., Zou, Z., Li, X., Li, H., Guo, Q., Yan, C., Tan, S. (2017). Experimental studies on the effects of green space and evapotranspiration on urban heat island in a subtropical megacity in China. *Habitat International, 68*, 30–42.
34. Roy, P.S., Ramachandran, R.M., Paul, O., Thakur, P.K., Ravan, S., Behera, M.D., Sarangi, C., Kanawade, V.P. (2022). Anthropogenic land use and land cover changes-a review on its environmental consequences and climate change. *Journal of the Indian Society of Remote Sensing, 508*, 1615–1640.
35. Silva, J.S., Silva, R.M.D., Santos, C.A.G. (2018). Spatiotemporal impact of land use/land cover changes on urban heat islands: A case study of Paço do Lumiar, Brazil. *Building and Environment, 136*, 279–292.
36. Singh, P., Kikon, N., Verma, P. (2017). Impact of land use change and urbanization on urban heat island in Lucknow city, Central India. A remote sensing based estimate. *Sustainable Cities and Society, 32*, 100–114.
37. Solecki, W.D., Rosenzweig, C., Parshall, L., Pope, G., Clark, M., Cox, J., Wiencke, M. (2005). Mitigation of the heat island effect in urban New Jersey. *Global Environmental Change Part B:*

Environmental Hazards, 6, 39–49.

38. Song, Y., Zenou, Y. (2012). Urban villages and housing values in China. *Regional Science and Urban Economics, 423*, 495–505.
39. Susca, T., Gaffin, S.R., Dell Osso, G.R. (2011). Positive effects of vegetation: Urban heat island and green roofs. *Environmental Pollution, 159*, 2119–2126.
40. Tian, L., Li, Y.C., Lu, J., Wang, J. (2021). Review on urban heat island in China: Methods, its impact on buildings energy demand and mitigation strategies. *Sustainability, 132*, 762.
41. United Nations Human Settlements Programme. (2023). Unlocking the Potential of Cities: Financing Sustainable Urban Development: Nairobi, Kenya: *UN - HABITAT*.
42. Wang, G., Guan, D. (2012). Effects of vegetation cover and normalized difference moisture index on thermal landscape pattern: A case study of Guangzhou, South China. *Chinese Journal of Applied Ecology, 239*, 2429–2436.
43. Wang, G., Zhang, Q., Xiao, R., Guan, D. (2017a). Urban thermal island regulated by green spaces——A case study of Guangzhou. *Ecological Science, 361*, 170–176.
44. Wang, G., Zhang, Q., Xiao, R., Guan, D. (2018). *Thermal island regulation differences of urban green spaces between autumn and winter in Guangzhou, South China*. Acta Scientiarum Naturalium Universitatis Sunyatseni, 575, 38–48.
45. Wang, S.Q., Sun, Q.C., Huang, X., Tao, Y.G., Dong, C.Y., Das, S., Liu, Y. (2023). Health-integrated heat risk assessment in Australian cities. *Environmental Impact Assessment Review, 102*, 107176.
46. Wang, S.Y., Ou, H.Y., Chen, P.C., Lin, T.P. (2024). Implementing policies to mitigate urban heat islands: Analyzing urban development factors with an innovative machine learning approach. *Urban Climate, 55*, 101868.
47. Wang, Y., Zhao, Y., Han, L., Ao, Y., Cai, J. (2017b). Coupling relationship of landscape pattern and urban heat island effect in Xi'an,China. *Chinese Journal of Applied Ecology, 288*, 2621–2628.
48. Wei, L.C., Duan, W., Dong, S.Q. (2024). Research on leased space of urban villages in large cities based on Fuzzy Kano Model evaluation and building performance simulation: A Case study of Laojuntang Village, Chaoyang District, Beijing. *Buildings, 141*, 120.
49. Weng, Q. (2003). Fractal analysis of satellite-detected urban heat island effect. *Photogrammetric Engineering & Remote Sensing, 695*, 555–566.
50. Windahl, E., de Beurs, K. (2016). An intercomparison of Landsat land surface temperature retrieval methods under variable atmospheric conditions using in situ skin temperature. *International Journal of Applied Earth Observation and Geoinformation, 51*, 11–27.
51. Xu, C., Li, L., Wang, J. (2015). Heat island effect mitigation by urban green space system: A case study of Taizhou City. *Ecology and Environmental Sciences, 244*, 643–649.
52. Xu, X., Cai, H., Qiao, Z., Wang, L., Jin, C., Ge, Y., Wang, L., Xu, F. (2017b). Impacts of park landscape structure on thermal environment using QuickBird and Landsat images. *Chinese Geographical Science, 5*, 818–826.
53. Xu, Z., Crooks, J.L., Black, D., Hu, W., Tong, S. (2017a). Heatwave and infants' hospital admissions under different heatwave definitions. *Environmental Pollution, 229*, 525.
54. Yu, G.T., Liu, T.W., Wang, Q., Li, T., Li, X.J., Song, G.H., Feng, Y.G. (2022). Impact of land use/land cover change on ecological quality during urbanization in the lower Yellow River Basin: A case study of Jinan City. *Remote Sensing, 1424*.
55. Yuan, S.H., Ren, Z.G., Shan, X.F., Deng, Q.L., Zhou, Z. (2023). Seasonal different effects of land cover on urban heat island in Wuhan's metropolitan area. *Urban Climate, 49*, 101547.
56. Yue, W.Z., Xue, L. (2016). Assessment on heat island effect based on urban regulatory planning. *Chinese Journal of Applied Ecology, 2711*, 3631–3640.
57. Zhang, Y.J., Zheng, S.Q., Song, Y., Zhong, Y.G. (2016). The spillover effect of urban village removal on nearby home values in Beijing. *Growth and Change, 471*, 9–31.
58. Zhang, J., Zhang, H.N., Qi, R.M. (2024). A study of size threshold for cooling effect in urban parks and their cooling accessibility and equity. *Scientific Reports, 14*, 16176.
59. Zhang, Z., Meng, J. (2013). Planning research of cooling channel in cities based on urban heat is land effect -on the case of Guangzhou. *Resources Science, 356*, 1261–1267.
60. Zheng, J., Li, Z.L., Zheng, B.H. (2024). A study on the effect of green plot ratio (GPR) on urban heat island intensity and outdoor thermal comfort in residential areas. *Forests, 15*(3), 518.
61. Zhou, X.F., Chen, H. (2018). Impact of urbanization-related land use land cover changes and urban morphology changes on the urban heat island phenomenon. *Science of the Total Environment, 635*, 1467–1476.
62. Zhu, Y.X., Zhang, Y.J., Li, Y., Zheng, Z.T., Zhao, G., Sun, Y.H., Gao, J., Chen, Y., Zhang, J.S., Zhang, Y. (2023). Human activities further amplify the cooling effect of vegetation greening in Chinese drylands. *Agricultural and Forest Meteorology, 342*, 109703.
63. Zou, Z.D., Yan, C.H., Yu, L.Y., Jiang, X.C., Ding, J.S., Qin, L.J., Wang, B., Qiu, G.Y. (2021). Impacts of land use/ land cover types on interactions between urban heat island effects and heat waves. *Building and Environment, 204*, 108138.